Supplementary Information

The structure-energy landscape of NMDA Receptor gating

Drew M. Dolino[1,2], Sudeshna Chatterjee[3], David M. MacLean[1], Charlotte Flatebo[3], Logan D.C. Bishop[3], Sana A. Shaikh[1], Christy F. Landes[3,4]*, and Vasanthi Jayaraman[1,2]*

[1] Center for Membrane Biology, Department of Biochemistry and Molecular Biology, University of Texas Health Science Center at Houston, Houston, Texas 77030, USA.

[2] Biochemistry and Molecular Biology Graduate Program, Graduate School of Biomedical Sciences, University of Texas Health Science Center at Houston, Houston, Texas, 77030, USA.

[3] Department of Chemistry, Rice University, Houston, Texas 77251, USA.

[4] Department of Electrical and Computer Engineering, Rice University, Houston, Texas 77251, USA.

*Correspondence to: Vasanthi Jayaraman, Department of Biochemistry and Molecular Biology, Center for Membrane Biology, University of Texas Health Science Center, MSB 6.528, 6431 Fannin St, Houston, Texas 77030 Tel.: (713) 500-6236, email: vasanthi.jayaraman@uth.tmc.edu; Christy F. Landes, Department of Chemistry, Rice University, Houston, TX Tel.: (713) 348-4232, email: cflandes@rice.edu.

Supplementary Results

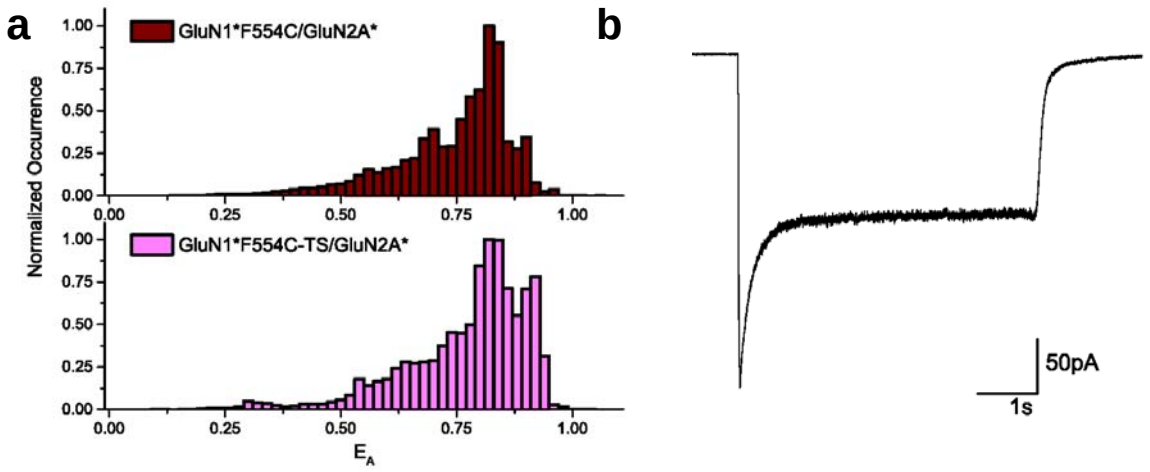

Figure 1.

(a) Comparison of glutamate-glycine bound NMDA receptor smFRET histograms when pulled down *via* immunoprecipitation (top) *vs* direct binding of streptavidin to an engineered Twin-Strep-tag (bottom). (b) Representative whole-cell trace of GluN1*F554C-TS/GluN2A* showing activation of receptor upon glutamate and glycine application. GluN1*F554C-TS/GluN2A* receptors desensitized to 42 ± 9 % with a time constant of 190 ± 50 ms (n=4).

Supplementary Results

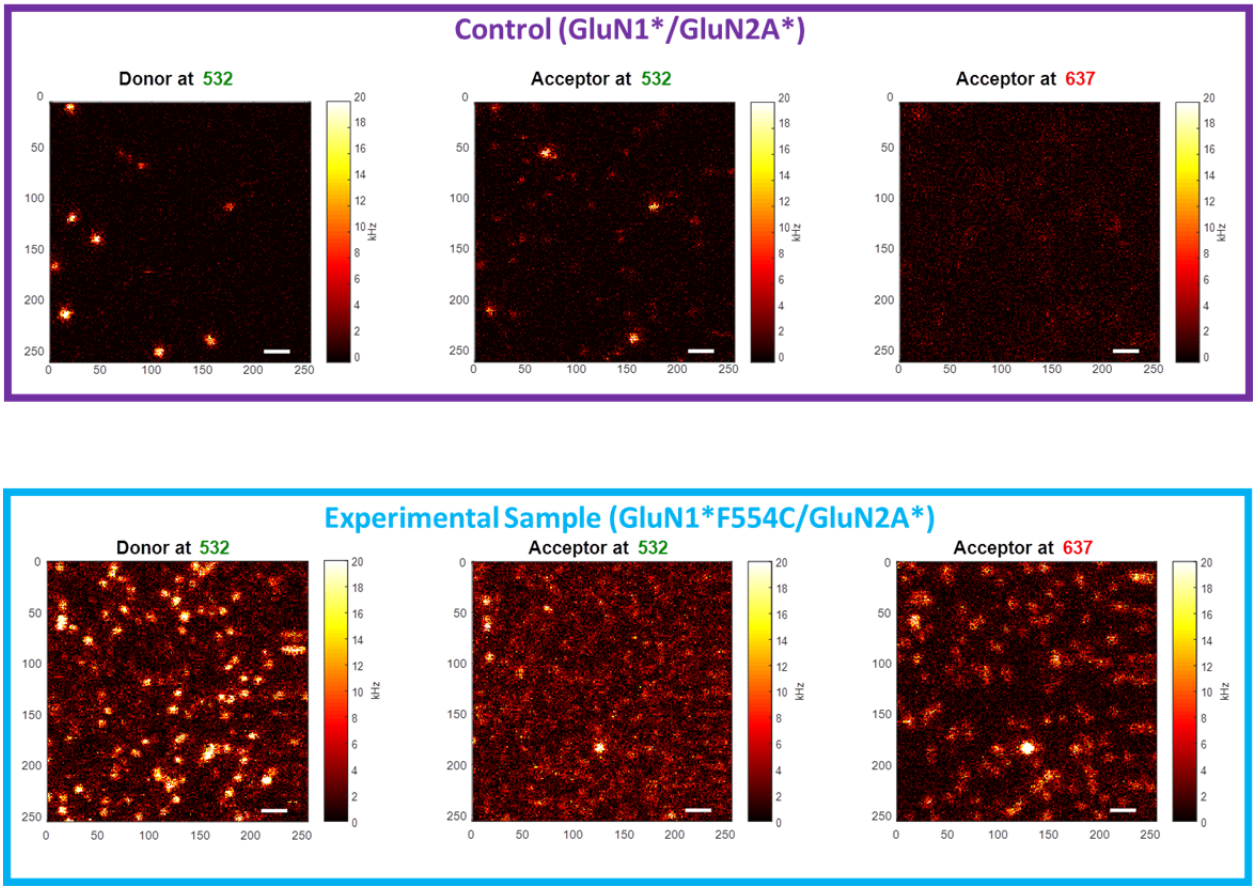

Figure 2.

Control slides showing minimal nonspecific fluorescence when examining control samples with labeling cells expressing background NMDA receptors without the F554C mutant (top panel) and with FRETting single molecules containing the F554C construct. Left panels show donor channel signal upon donor excitation at 532 nm, middle panels show acceptor channel signal upon donor excitation (FRET signal), and right panels show acceptor channel signal upon direct excitation of the acceptor at 637 nm.

Supplementary Results

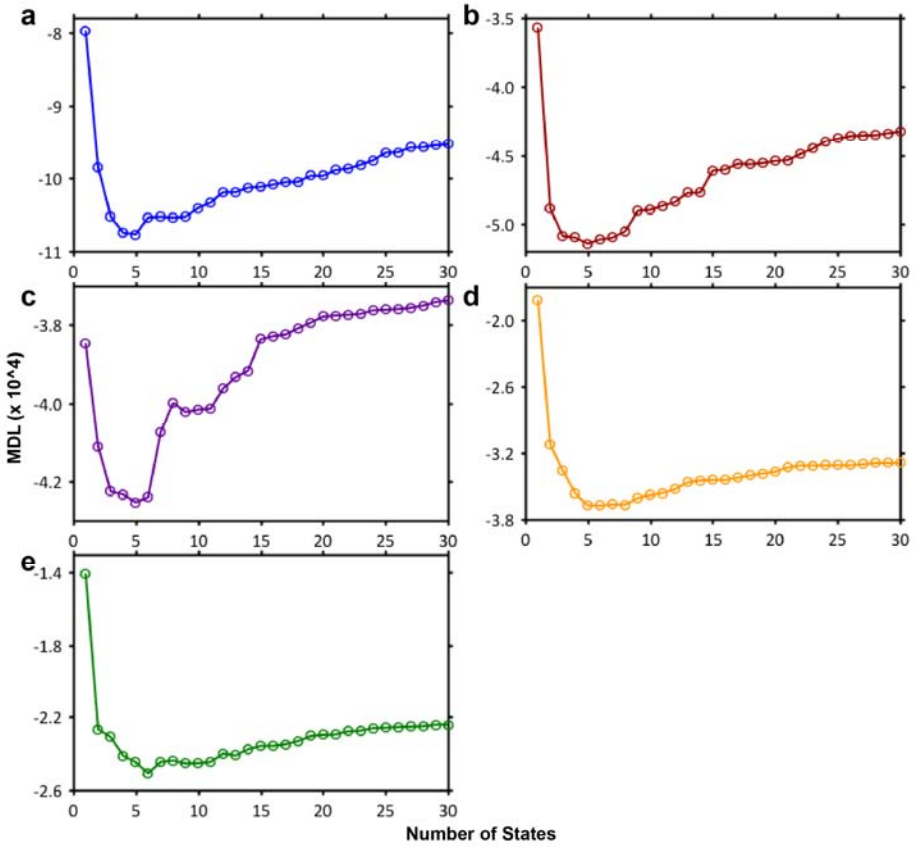

Figure 3

Minimum Description Length (MDL) plots for each liganded condition used during STaSI analysis. In determining the correct number of states to apply to each dataset, the MDL function is used to quantify the appropriateness of a model by considering both the goodness of the fit (which lowers the value as goodness increases) and its complexity (which increase the value as complexity increases) simultaneously. The number of states that allows the MDL function to reach its minimum is taken as the most appropriate model that balances simplicity and accuracy. Shown here are the MDL plots for (a) apo, (b) glutamate-glycine, (c) glutamate-glycine/Zn^{2+}, (d) glutamate-glycine and 50 μM MK-801, and (e) glutamate-glycine and 1 μM MK-801.

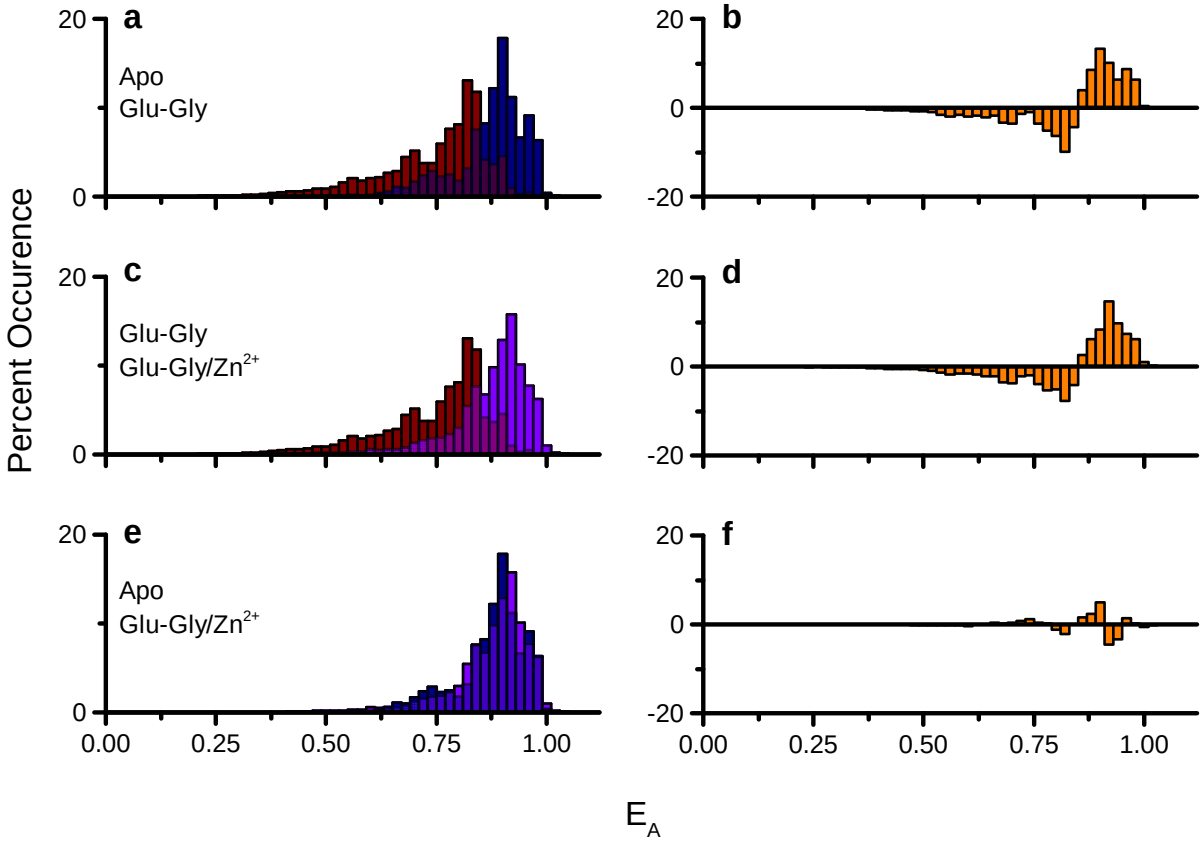

Figure 4.

Difference histograms clarify the changing conformational landscape of the NMDA receptor as it shifts between inactive and active conditions. Parent denoised FRET efficiency distribution histograms were paired and subtracted from one another to generate difference histograms. The positive/negative value of the difference histogram signifies higher/lower relative abundance of one condition as compared to the other. Shown are the parent and difference histograms for apo vs. glutamate-glycine-bound receptor (**a and b**), glutamate-glycine vs. glutamate-glycine with zinc (**c and d**), and apo vs. glutamate-glycine with zinc (**e and f**).

Supplementary Results

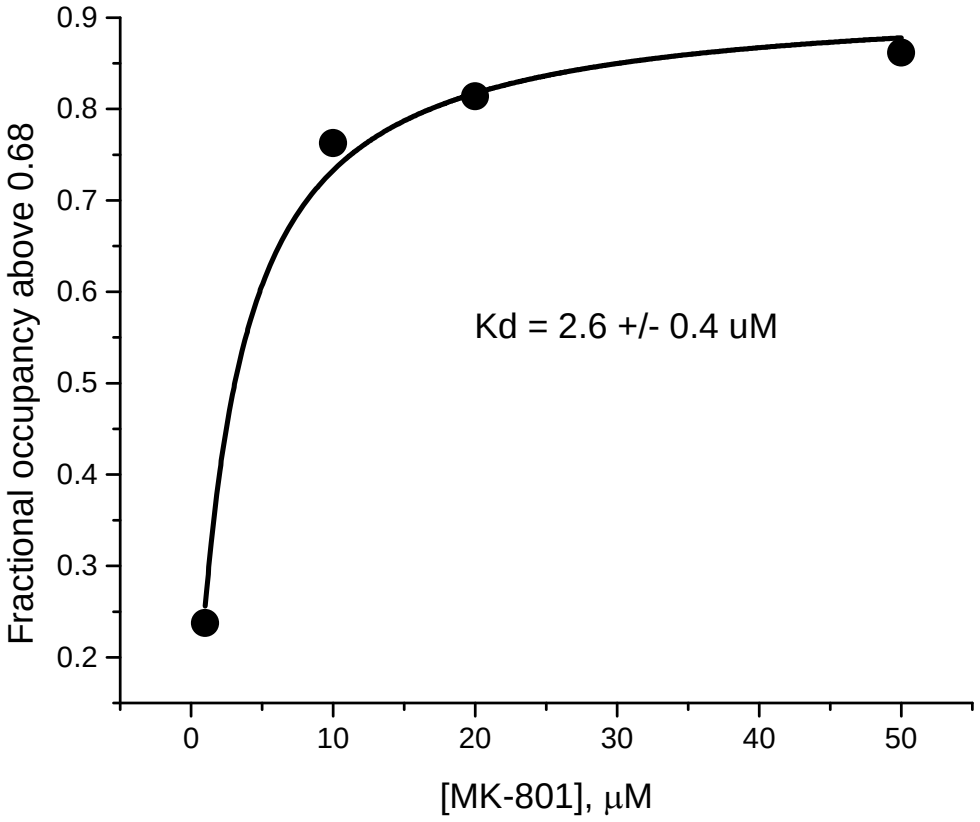

Figure 5.

Dose Response curve for trapping of MK-801. The fraction of GluN1*F554C/GluN2A* receptors exhibiting an efficiency of 0.68 or higher was plotted against the MK-801 concentration. Above the efficiency of 0.68, we assume bound receptors to have trapped MK-801 in the pore by closing upon it, while efficiencies below 0.68 are assumed to have an open channel conformation.

Supplementary Results

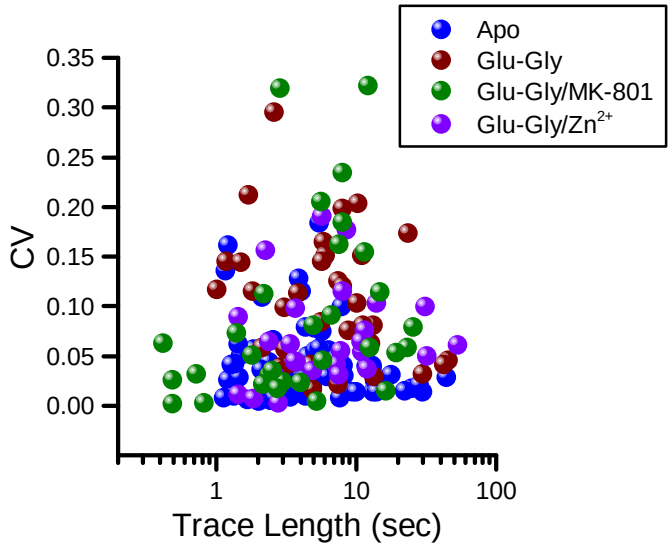

Figure 6.

The coefficient of variation (CV) of each smFRET efficiency trajectory versus that trajectory's length. Having various lengths of the smFRET trajectories does not affect the CV-ligand condition relationship.

Supplementary Results

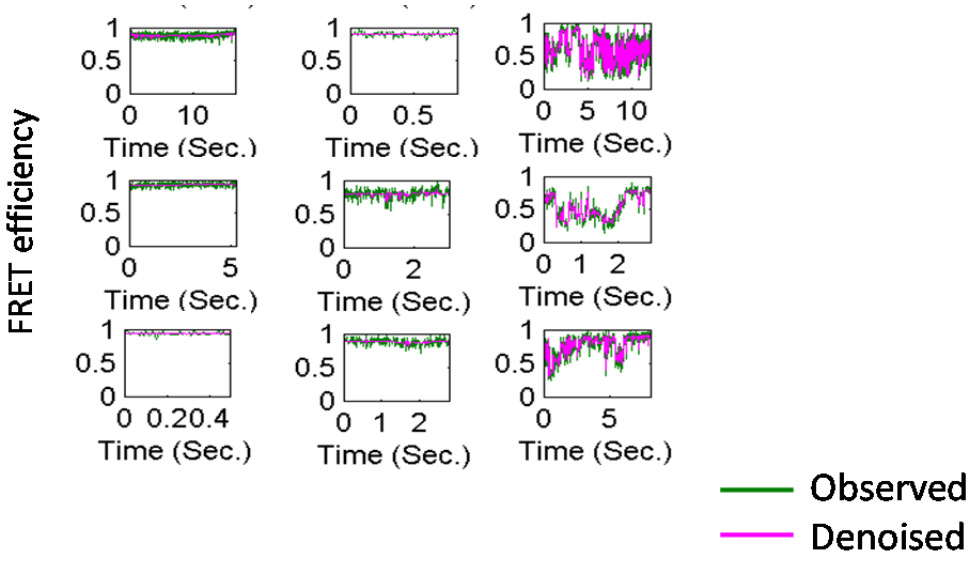

Figure 7.

Representative smFRET traces from 9 MK-801 bound receptor molecules in the presence of glutamate and glycine. Two main populations are shown: low-FRETting molecules showing large transitions and high FRETting molecules that are stable with very few transitions.